Sensors and Materials, Vol. 15, No. 1 (2003) 037–042
MYU Tokyo

S & M 0507

Evolution of Surface Roughness in KOH Etching of Silicon Caused by Material Defects

Eero Haimi and Veikko K. Lindroos

Laboratory of Physical Metallurgy and Materials Science
Helsinki University of Technology, P.O.Box 6200, 02015 HUT, Finland

(Received September 30, 2002; accepted January 14, 2003)

Key words: silicon, KOH etching, surface roughness, material defects

In the absence of pyramidal hillocks, a typical (100) surface morphology of KOH etched silicon builds up from shallow pits. Recently, contradictory experimental results have been reported on the role of thermal history and oxygen concentration of silicon on surface roughness. In the present work, the evolution of the (100) surface roughness in KOH etching of silicon has been studied in order to clarify the origin of the roughness. In the experiments, bulk microdefect density of p+-type silicon wafers was measured and, thereafter, the wafers were etched using different etching times. Comparison of the results supports the idea that material defects act as sources of etching defects on the (100) silicon surface.

1. Introduction

Anisotropic etching of single-crystal silicon in aqueous KOH solutions is a technically important process in silicon micromachining. Recently, surface roughness of silicon after etching has gained much attention, because microsystem devices have become so small that surface roughness of etched silicon is starting to affect the dimensional accuracy of final component structures.

Surface roughness may comprise various elements such as notching effects, pyramidal hillocks, pits and atomic roughness depending on the length scale under consideration. Much work has been devoted to clarify the influence of processing conditions on surface roughness. Processing parameters such as KOH consentration,[1–3] temperature,[1–3] time,[1–3]

pressure,[4] contamination,[5–8] stirring,[1] dissolved gases,[4,7,9] anodic bias,[10,11] and surfactant additions[12] have been studied. A major research subject has been the formation of pyramidal hillocks. According to the literature, pyramidal hillocks can be avoided when high-purity water and KOH as well as proper processing conditions are utilized.[7,8,13] In the absence of pyramidal hillocks, a typical (100) surface morphology of KOH-etched silicon builds up from shallow pits.[14]

The influence of silicon on surface roughness has also attracted attention. Normally, Cz-grown silicon crystals are supersaturated with oxygen after crystal pulling. During subsequent annealing, oxygen precipitates and, in some cases, process-induced stacking faults and dislocations are created. Precipitates have been claimed to produce a pseudomasking effect in anisotropic wet chemical etching and subsequent hillock formation,[13] but this is not unanimously accepted. However, it is well known that precipitates, and other bulk microdefects as well, are sensitive to anisotropic wet etching. This is utilized in several standardized defect etchants such as the ones named after Dash, Stirtl, Secco, Wright, Schimmel, and Yang.[15] Accordingly, an influence of thermal history and oxygen concentration on the quality of KOH etched (100) silicon surfaces has been recently reported.[16] However, contradictory experimental results, where no clear dependence of the surface roughness on the oxygen concentration of silicon and thermal processing of the samples, have also been reported.[17]

In the present work the evolution of the (100) surface roughness in KOH etching of silicon has been studied in order to clarify the origin of the roughness.

2. Experimental

In the experiments, boron-doped, low-oxygen-content p+-type (100) silicon wafers were etched without patterning. A low oxygen content (8 ppm level) was selected in order to have moderate defect density. The wafers were manufactured from the same crystal part, which ensured narrow material property deviation. Moreover, to assure depth homogeneity, the wafers were used in the as-received condition as far as the thermal history was concerned. This prevented formation of denuded zones. Before the etching, the bulk microdefect density (BMD) of the wafers was measured using a scanning infrared microscope (SIRM); the instrument used was Semilab SIRM-300. The technique is based on confocal reflection mode arrangement and infrared scattering from defects. With the method, it is possible to capture images nondestructively from the desired depth below the sample surface. Detailed information on SIRM technique is available in refs. 18 and 19. The etching was performed in 30 wt% aqueous KOH solution at 75°C. Twelve wafers were etched utilizing different etching times. The etching times were 0.16, 1, 5, 10, 15, 20, 25, 30, 45, 60, 75, and 112 min, which correspond to approximate etching depths of 0.2, 0.7, 4, 7, 10, 14, 17, 21, 31, 41, 52, and 78 μm, respectively. Depth estimates were subsequently calculated from mass reduction. The etching solution was obtained by mixing high purity KOH pellets (Merck's p.a. quality) and DI water.

Surface roughnesses of the etched (100) surfaces were studied using Nomarsky-type optical microscope. For each wafer, four images were taken from both sides. The images were analyzed by calculating etch pit densities.

3. Results and Discussion

The roughness of the etched surfaces consisted of shallow pits. It can be seen from Fig. 1, that the characteristic surface roughness developed in the time scale of hours. This suggests that the roughness does not originate from hydrogen evolution, since the time scale of hydrogen bubble formation and detachment is a couple of seconds. Furthermore,

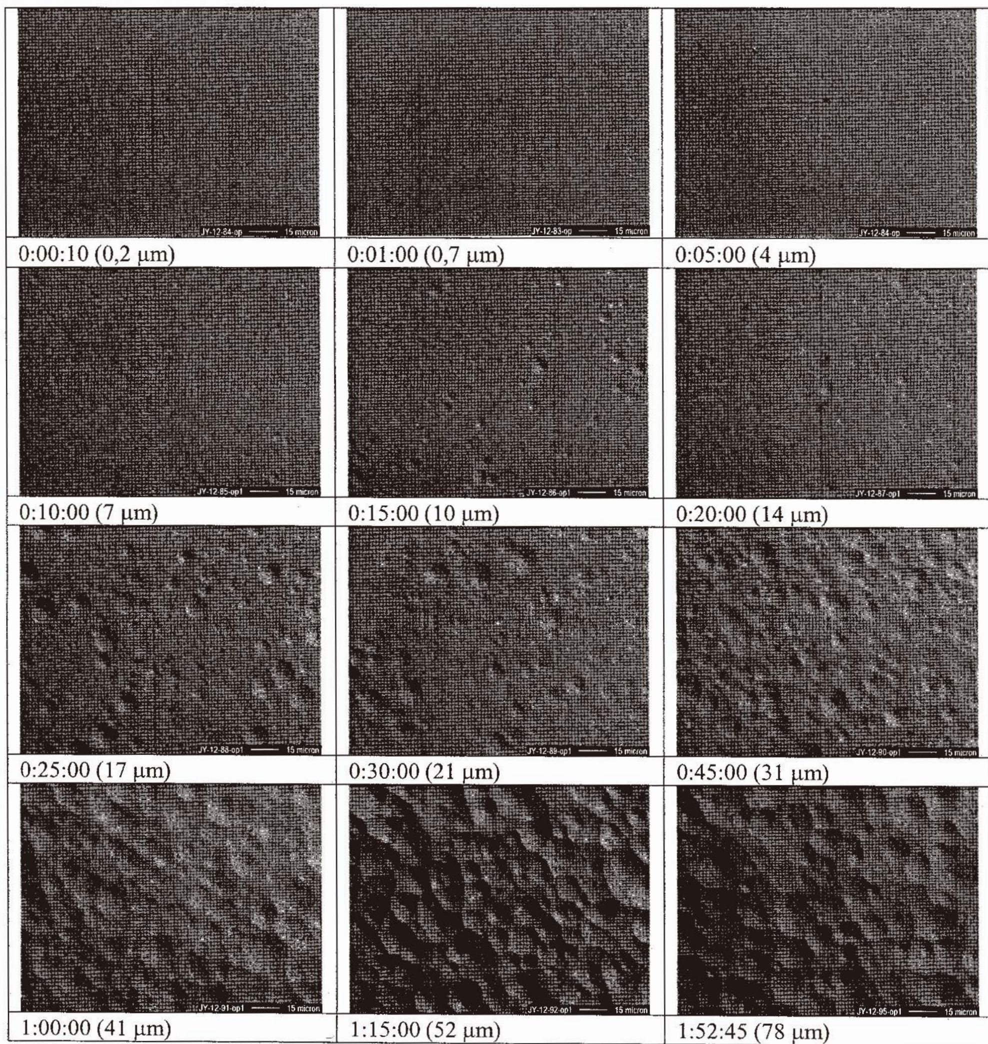

Fig. 1. Evolution of surface roughness of KOH-etched silicon as a function of etching time.

localization of hydrogen evolution is not a plausible explanation either, because localization of a cathodic reaction would imply hillock formation rather than pit formation.

The etch rate of silicon is enhanced in the pit area. In order to characterize the pitting, the number etch pits were calculated from microscope images giving directly areal pit density estimates. Since KOH is an anisotropic etchant, it does not smooth the surface in the applied experimental conditions. Consequently, areal pit density can be regarded as an integral of events occurring during the etching. Assuming that the pits are caused by defects in silicon crystals similarly to standard defect etching, several estimates of bulk defect density can be attained from the experimental data of areal pit densities corresponding to dissimilar etching depths. Respective areal density of pits is just divided by the etching depth and results corresponding to different etching depths represents different sampling volumes. However, in case of etching depths deeper than 30 μm, overlapping of pits starts to occur and, therefore, this data is not typical. An independent estimate of BMD is attained from SIRM defect depth profile measurements. In this case data near the wafer surface (closer that 10 mm) is not typical due to surface reflection of the laser beam. Furthermore, it should be emphasized that SIRM measurements do not differentiate between oxygen precipitates and large vacancy clusters as bulk microdefects.

In Fig. 2. the results from both KOH etching and SIRM measurements have been plotted in logarithmic coordinates. Utilizing the shorter etching time part of the data, the density of defects derived from pitting is estimated to be on the order of 2×10^8 defects per cubic centimeter with 35% coefficient of variation. Defect density obtained from SIRM measurement is on the order of 2×10^7 defects per cubic centimeter with 30% coefficient of variation. The SIRM result is considerably lower than the pit calculation result.

The time scale of shallow pit formation during KOH etching supports the assumption that the pits originate from material defects. The difference between the bulk microdefect

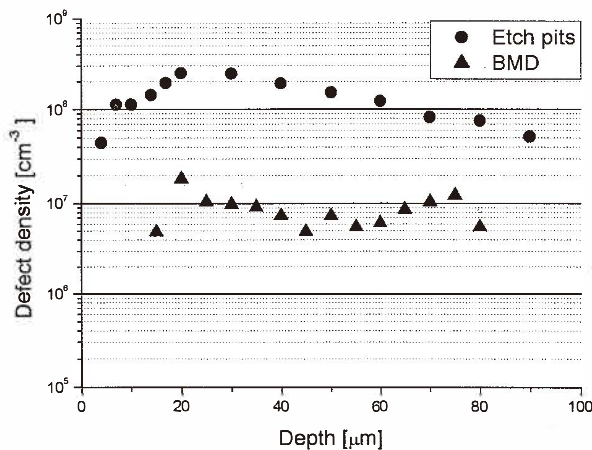

Fig. 2. Defect densities based on pit calculations and SIRM measurements.

density measurement with SIRM and the pit calculation measurements could be explained by assuming that the defects initiating the pits are very small and substantial parts of them fall below the detection limit of SIRM. According to the literature, SIRM detects oxide precipitates larger than approximately 50 nm.[19] In any case, the results do not support the interpretation that the pits originate from stacking faults or punched-out dislocations. In such a case, pit calculation should give lower defect numbers than SIRM measurements, since bulk stacking faults and punched out dislocations are precipitate-induced defects and only a part of the precipitates induce other defects. Moreover, precipitates that induce defects belong typically to the large size proportion of precipitate distribution.

4. Conclusions

The results of the present study support the assumption that the shallow pits observed on (100) surfaces of silicon after KOH etching are caused by material defects. The differences in the two defect density estimates obtained in the work may be explained as being due to differences in the resolution of the methods. It is possible that the smallest defects fall below the resolution limit of SIRM. The results are in accordance with the previously suggested idea that defects could act as velocity sources in etching of the (100) silicon surface.[20] However, further investigation is required in order to clarify the detailed characteristics of the proposed defects.

Acknowledgments

The authors would like to thank Mr. Sami Kaarlela and Mr. Kalevi Vanhatalo for their contribution to the experimental work. Furthermore, the authors are grateful to the Academy of Finland for the funding support.

References

1 E. D. Palik, O. J. Glembocki, I. Hear Jr., P. S. Bruno and L. Tenerz: J. Appl. Phys. **70** (1991) 3291.
2 G. Findles, J. Muchow, M. Koch and H. Munzel: Proceedings of the IEEE Conference on Micro Electro Mechanical Systems (IEEE 1992) p. 62.
3 K. Sato, M. Shikida, T. Yamashiro, M. Tsunekawa and S. Ito: Sensors and Actuators A **73** (1999) 122.
4 A. P. Abbot, S. A. Campbell, J. Satherley, and D. J. Schiffrin: J. Electroanal. Chem. **348** (1993) 473.
5 T. A. Kwa and R. F. Wolffenbuttel: J. Micromech. Microeng. **5** (1995) 95.
6 A. Hein, O. Dorsch and E. Obermeier: Transducers '97, International Conference on Solid-State Sensors and Actuators (IEEE 1997) p. 687.
7 S. A. Cambell, K. Cooper, L. Dixon, R. Earwaker, S. N. Port and D. J. Schiffrin: J. Micromech. Microeng. **5** (1995) 209.
8 H. Tanaka, Y. Abe, T. Yoneyama, J. Ishikawa, O. Takenaka and K. Inoue: Sensors and Actuators A **82** (2000) 270.
9 P. M. M. C. Bressers, J. J. Kelly, J. G. E. Gardeniers, and M. Elwenspoek: J. Elecrochem. Soc. **143** (1996) 1744.

10 E. D. Palik, V. M. Bermudes and O.J . Glembocki: J. Electrochem. Soc. **132** (1985) 871.
11 R. S. Hutton, S. N. Port, D. J. Schiffrin and D. E. Williams: J. Elecroanal. Chem. **418** (1996) 153.
12 R. Divan, N. Moldovan and H. Camon: Sensors and Actuators A **74** (1999) 18.
13 M. Matsuoka, Y. Yosihida, and M. Moronuki: J. Chem. Eng. Japan 25 (1992) 735.
14 E. van Veenendaal, K. Sato, M. Shikida, and J. van Suchtelen: Sensors and Actuators A **93** (2001) 219.
15 ASTM Standard F 1809-97
16 A. Hein, S. Finkbeiner, J. Marek and E. Obermeier: Sensors and Actuators A **86** (2000) 86.
17 T. Muller, G. Kissinger, A.C. Benkitsch, O. Brand and H. Baltes: J. Electrochem. Soc. **147** (2000) 1604.
18 G. R. Booker, Z. Laczik, and P. Kidd: Semicond. Sci. Technol. **7** (1992) 110.
19 P. Török and L. Mule'stagno: J. Microscopy **188** (1997) 1.
20 E. van Veenendaal, K. Sato, M. Shikida, A. J. Nijdam and J. van Suchtelen: Sensors and Actuators A **93** (2001) 232.